



Pentaarylbiimidazole, PABI: An Easily Synthesized Fast Photochromic Molecule with Superior Durability

Journal:	<i>ChemComm</i>
Manuscript ID:	CC-COM-04-2014-003137.R1
Article Type:	Communication
Date Submitted by the Author:	14-May-2014
Complete List of Authors:	Yamashita, Hiroaki; Aoyama Gakuin University, Department of Chemistry, School of Science and Engineering Abe, Jiro; Aoyama Gakuin University, Department of Chemistry, School of Science and Engineering

COMMUNICATION

Pentaarylbiimidazole, PABI: An Easily Synthesized Fast Photochromic Molecule with Superior Durability

Cite this: DOI: 10.1039/x0xx00000x

Hiroaki Yamashita^a and Jiro Abe^{*ab}Received 00th January 2012,
Accepted 00th January 2012

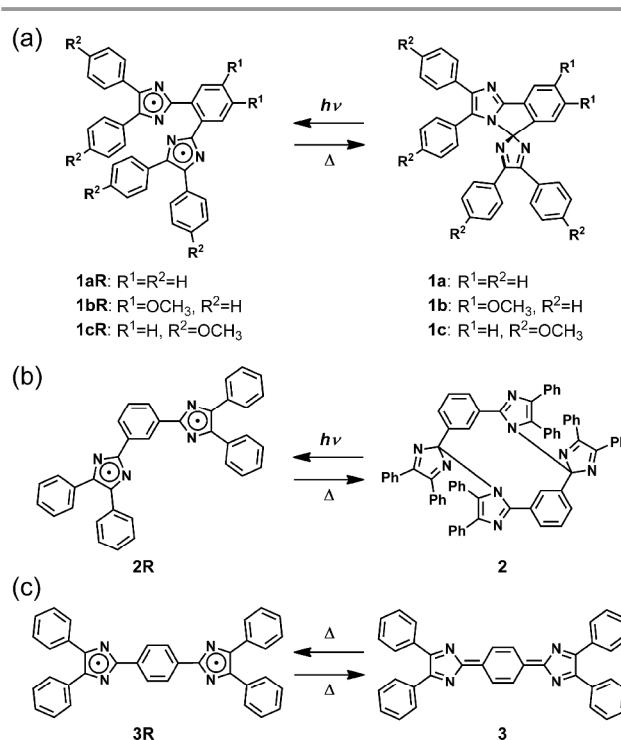
DOI: 10.1039/x0xx00000x

www.rsc.org/

We report a new type of fast photochromic imidazole dimer, pentaarylbiimidazole (PABI), which shows a few μ s fast photochromism with high fatigue resistance against light irradiation. PABI has an unusual spiroconjugated imidazoisindole skeleton and its derivatives can be prepared by simple synthetic procedures.

Hexaarylbiimidazole (HABI) generates the colored radical species by UV light irradiation and the colored species gradually returns to the initial colorless imidazole dimer when light irradiation is stopped.¹⁻⁵ Inspired from the photochromism of HABI, we have developed the bridged imidazole dimers to accelerate the thermal back reaction.⁶⁻¹⁷ The bridged imidazole dimers show instantaneous coloration upon UV light irradiation and rapid fading in the dark. The half-lives of the colored species of the naphthalene-bridged imidazole dimer and the [2.2]paracyclophane-bridged imidazole dimer are 830 and 33 ms at 25 °C in benzene, respectively.^{8,16,17} Such fast photochromic molecules could be served as excellent probes and triggers to reveal and control phenomena which occur under the time scales within a few tens of ms. The fast photochromic molecules have potentials for the applications such as a holographic display and fluorescence switching.¹⁸⁻²⁰ We have broadened the photochromic properties such as the half-life and the color of the colored species by rational design of the bridged imidazole dimers.^{6,15} However, the complicated synthesis procedures and costly compounds have been making them the subject of potential for widely applicable molecular switching systems. In fact, the commonly used photochromic compounds, diarylethenes, azobenzenes, spiropyrans and naphthopyrans, are easily accessible to many researchers.

The simplest architecture to incorporate a couple of imidazolyl radicals into a molecule is achieved by using the phenylene group as a linker of the imidazolyl radicals. The design of a novel photochromic imidazole dimer **1a**,



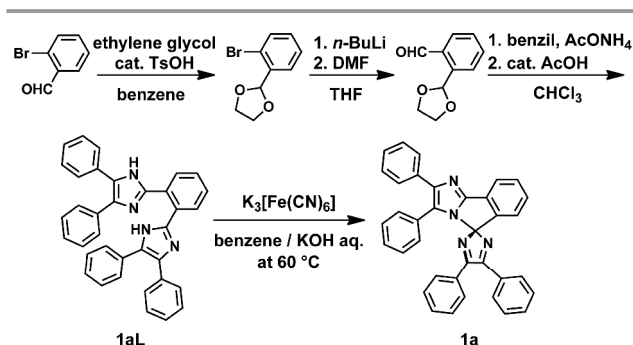
Scheme 1 Photochromism of (a) **1a**, **1b**, **1c**, (b) **2**, and (c) Thermal Equilibrium between **3** and **3R**

pentaarylbiimidazole (PABI), in Scheme 1a, was initially motivated by the characteristic behavior of its structural isomers, 2,2'-(*m*-phenylene)bis(4,5-diphenyl-1-imidazolyl) (**2R**)^{21,22} and 1,4-bis(4,5-diphenylimidazole-2-ylidene)cyclohexa-2,5-diene (**3**)²³⁻²⁵. The π -electronic structures of **1aR**, **2R**, and **3R** are considered to be topologically equivalent to those of *o*-, *m*-, and *p*-quinodimethanes (*o*-, *m*-, and *p*-QDMs), respectively.^{26,27} The spin states of *o*-, *m*-, and *p*-QDMs obey well-known

Ovchinnikov's rule.²⁸ *o*- and *p*-QDMs have the singlet ground state and *m*-QDM has the triplet ground state as predicted by Ovchinnikov's rule. Thus, QDMs are important as the fundamental model to understand the nature of the organic biradicals. Besides, QDMs are attractive not only in the field of physical chemistry but also in synthetic chemistry.²⁹⁻³¹ The QDMs are highly reactive and undergo the dimerization or polymerization characteristic to radicals.³² However, it is notable that only *o*-QDM undergoes intramolecular cyclization to form the benzocyclobutene.¹⁵ Thus we came up with an idea that **1aR** would form a new type of imidazole dimer **1a** by the intramolecular radical recombination.

We previously reported the theoretical investigation for the electronic structure of **3R** which possesses the singlet ground state and thermally accessible triplet biradical state.²⁴ Moreover, the fluorinated derivative of **3R**, where four hydrogen atoms at the central phenylene ring are substituted with four fluorine atoms, has pronounced biradical character and shows the intermolecular radical dimerization reaction to form the colorless imidazole dimer.³⁴ The *m*-isomer **2R** also causes the intermolecular radical dimerization reaction to lead the formation of **2**.^{21,22} The spin state of the ground state of **2R** was assigned to the triplet biradical state by ESR analysis as would be predicted by Ovchinnikov's rule. These results suggest that the spin states of the ground states of **2R** and **3R** are governed by the topology of the π -electron system in the same manner as QDMs. Consequently, the singlet ground state can be predicted for the ground state of **1aR** from the analogy with *o*-QDM. It is of great interest that not only the through-bond but also the through-space radical-radical interactions play important role in the spin state of **1aR** due to the closely spaced imidazolyl radicals. In other words, the competition between the formation of σ -bond and π -bond in **1aR** would be expected. Thus **1a** is attractive target for understanding the biradical chemistry and the bond formation and breaking processes. In this paper, we developed a photochromic imidazole dimer PABI, **1a** and its methoxy substituted derivatives, **1b** and **1c** (Scheme 1). PABI derivatives are easy to prepare compared with so far developed bridged imidazole dimers. We investigated the electronic structures of the colored species of PABI derivatives by nanosecond laser flash photolysis and ESR measurements. We found that the half-lives of the colored species of PABI derivatives are drastically changed by introducing the methoxy groups on the phenylene group.

The precursor (**1aL**) was prepared by three steps from the starting material, 2-bromobenzaldehyde (Scheme 2). A key step of the synthetic scheme is the synthesis of **1aL** from asymmetrically protected *o*-phthalaldehyde (2-(1,3-dioxolan-2-yl)benzaldehyde)³⁵ because the direct synthesis of **1aL** from *o*-phthalaldehyde was unsuccessful due to the side reactions. The target compound (**1a**) was obtained by the oxidation of the precursor with aqueous potassium ferricyanide in basic condition. The single crystal of **1a** suitable for the X-ray crystallographic analysis was obtained by recrystallization from hexane/dichloromethane. The ORTEP representations of the molecular structures of **1aL** and **1a** are shown in Fig. 1. The



Scheme 2 Synthetic scheme of PABI

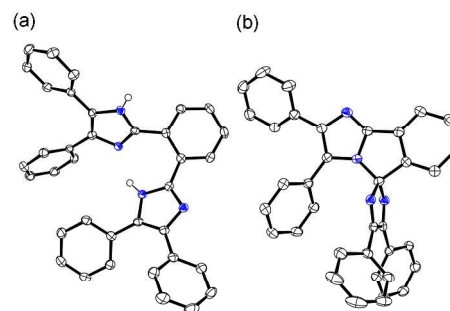


Fig. 1 ORTEP representations of the molecular structures of (a) **1aL** and (b) **1a** with thermal ellipsoids (50% probability), where nitrogen atoms are highlighted in blue.³⁶

molecular structure of **1a** is unusual and different from previously reported bridged imidazole dimers. The main skeleton of **1a** is the spiroconjugated^{37,38} 5*H*-imidazo[2,1-*a*]isoindole. The imidazoisoindole moiety and the imidazole ring are almost perpendicular orientation. The C–N bond length between the two imidazole rings of **1a** (1.459 Å) is the shortest value in HABI derivatives reported so far owing to the spiroconjugation. For example, the C–N bond length of [2.2]paracyclophane bridged imidazole dimer, *pseudogem*-bisDPI[2.2]PC, is 1.488 Å.¹⁶

The photochromic behavior of HABI is described by the photoinduced homolytic cleavage of the C–N bond between the imidazole rings and the thermal radical recombination.^{4,5} It is necessary to confirm whether the photochromic reaction of PABI proceeds by the same mechanism as that of HABI because of its unusual molecular structure. We measured the ESR spectra of the benzene solution of **1a** at room temperature under UV irradiation (365 nm). The ESR signal characteristic to organic radicals was observed under irradiation (Fig. S31) and instantly disappeared when light irradiation was stopped. This observation is clear evidence that the photogenerated species **1aR** is a radical species with unpaired electrons. The temperature dependence of the ESR signal intensity provides the information about the spin state of **1aR**. The ESR signal intensity (I_{ESR}) of **1aR** increases with raising the temperature from -195 to -73 °C (Fig. S32), indicating that the colored species of **1a** has the singlet ground state and the population of the thermally excited

triplet state increases with increasing the temperature. This behavior is similar to the temperature dependence of the I_{ESR} of **3R**.²⁴ Therefore, the electron spins in **1aR** anti-ferromagnetically couple with each other. On the other hand, the I_{ESR} begins to decrease sharply due to the radical recombination to form the imidazole dimer **1a** by raising the temperature above -73 °C.

We also synthesized PABI derivatives that have the methoxy groups on the phenylene group (**1b**) and the four phenyl groups (**1c**). As compared with the previously reported bridged imidazole dimers, the readily synthetic procedure to introduce the substituents on the phenylene group is an attractive feature of PABI derivatives. As described above, the colored species of PABI derivatives, **1aR**, **1bR**, and **1cR**, have a significant contribution from the σ -QDM resonance form, indicating that two imidazolyl radicals are electronically coupled via the phenylene group. Hence, the significant variations of the photochromic properties are expected by introducing substituents on the phenylene group.

Transient absorption spectra of the colored species of PABI derivatives, **1a**, **1b**, and **1c** are shown in Fig. 2a. As can be expected from the large difference in the molecular structures, the spectral shapes of the colored species of PABI are quite different from those of previously reported bridged imidazole dimers. The remarkable features of these spectra are the intense absorption band in the 700–800 nm region. These absorption bands are attributable to the radical–radical interaction, which is supported by the TDDFT calculations (UB3LYP/6-31+G(d,p)) (Fig. S35). These intense bands indicate the existence of the stronger radical–radical interaction compared with the previously reported bridged imidazole dimers. The α - and β -spins in the colored species of the [2.2]paracyclophane bridged imidazole dimers are localized on each imidazole rings. In that case, through-space radical–radical interaction is dominant. On the other hand, the through-bond radical–radical interaction is considered to play an important role with regard to the colored species of PABI derivatives due to the spin delocalization from one imidazole ring to another ring via the phenylene group (Fig. S34). Furthermore, the singlet biradical index (γ) of **1aR** was estimated to be 29% from the LUMO occupation number by the CASSCF(8,8)/6-31G(d)/B3LYP/6-31+G(d,p) level of the theory.

The decay profiles at 25 °C of the colored species of PABI derivatives in benzene measured at 710 nm are shown in Fig. 2b. All decays follow the first-order kinetics and are well fitted with a single exponential function. The half-lives of **1aR**, **1bR**, and **1cR** are 2.0, 101, and 3.6 μ s at 25 °C, respectively. The thermal back

Table 1 Decoloration Reaction Rates, Half-Lives at 25 °C, and Activation Parameters of the Colored Species of **1a**, **1b**, and **1c** in Degassed Benzene

	k [s ⁻¹]	$\tau_{1/2}$ [μ s]	ΔH^\ddagger [kJ/mol]	ΔS^\ddagger [J/mol·K]	ΔG^\ddagger [kJ/mol]
1aR	3.5×10^3	2.0	35.4	-20.0	41.4
1bR	6.9×10^3	101	46.0	-16.8	51.0
1cR	1.9×10^5	3.6	37.7	-17.0	42.8

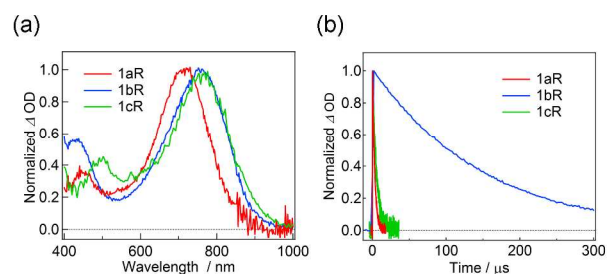


Fig. 2 (a) Transient absorption spectra of the colored species of **1a**, **1b**, and **1c** in degassed benzene. The spectral shapes do not change during the decay processes. (b) Decay profiles of the colored species of **1a**, **1b**, and **1c** in degassed benzene at 25 °C (excitation wavelength, 355 nm; pulse width, 5 ns; power 4 mJ/pulse; the concentrations of **1a**, **1b**, and **1c** are 3.1×10^{-4} M, 2.6×10^{-4} M, and 3.3×10^{-4} M, respectively).

reactions of PABI derivatives proceed in the μ s time scale. It is noteworthy that the half-life of the colored species is drastically changed by introducing the methoxy groups on the phenylene group. On the other hand, the half-life remains nearly unchanged when the methoxy groups are introduced on the phenyl groups. These results can be explained by the spatial distribution of the frontier molecular orbitals. The HOMO and LUMO of **1aR** are mainly located on the imidazole–phenylene–imidazole moiety (Fig. S33). Therefore, the introduction of either electron-donating or electron-withdrawing groups on the phenylene group are effective to alter the electronic structure of **1aR**. The LUMO of the **1a** is localized on the 2*H*-imidazole ring. Thus, only the colored species is stabilized by introducing the methoxy groups on the phenylene group, leading to the decrease in the change in Gibbs free energy, ΔG^0 , between the colored and colorless species. Consequently, increasing in the free energy of activation, ΔG^\ddagger , is expected from the linear free energy relationship. We conducted the measurements of the decay profiles in the temperature ranges between 5 and 40 °C and obtained the activation parameters (ΔH^\ddagger , ΔS^\ddagger , and ΔG^\ddagger) by using the Eyring equation (Table 1). No significant differences in ΔS^\ddagger were found between the derivatives, suggesting that structural changes from the colored species to the transition states are almost same in

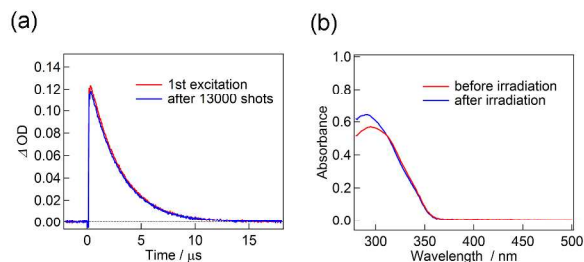


Fig. 3 (a) Decay profile of the colored species of **1a** at 25 °C in O₂ saturated benzene for the fresh sample and the sample after 13,000 shots of the 355 nm laser pulses (pulse width, 5 ns; power 4 mJ/pulse; the concentration 2.1×10^{-4} M). The half-life is estimated to be 2.0 μ s from the first-order plot of the decay profile. (b) UV-vis absorption spectra of **1a** in O₂ saturated benzene for the fresh sample and the sample after 13,000 shots of the 355 nm laser pulses.

1aR, **1bR**, and **1cR**. The difference in ΔG^\ddagger between **1aR** and **1bR** is attributable to the difference in ΔH^\ddagger . This result indicates that the introduction of the methoxy groups on the phenylene group affects the enthalpy term of ΔG^\ddagger . The high fatigue resistance against light irradiation is required for practical application. We evaluated the fatigue resistance of **1a**, **1b**, and **1c**. The decay profiles of the colored species and UV-vis absorption spectra of the colorless species were measured for the fresh samples and the samples after 13,000 shots of the 355 nm laser pulses (the pulse duration and the power is 5 ns and 4 mJ). No significant differences are found between the fresh samples and the laser-irradiated samples for all of the decay profiles and the spectra, indicating that PABI derivatives have high fatigue resistance (Figs. S17, S20, S22, S25, S27, S30). Furthermore, we confirmed that the presence of molecular oxygen has no influence on the half-life of the colored species of **1a** and only a slight influence on the fatigue resistance as shown in Fig. 3.

In conclusion, we developed a new type of fast photochromic imidazole dimer, PABI. PABI derivatives are easy to synthesize and show fast photochromism in μs time scale. It was revealed that the electronic structures of the colored species of PABI derivatives are similar to that of *o*-QDM. This is the first report of reversible generation of the *o*-QDM structure, which is an important species in physical and synthetic chemistry. We found that the introduction of the electron-donating methoxy groups on the phenylene effectively stabilizes the colored species, resulting in the prolonged half-life of the colored species **1bR**. Moreover, PABI derivatives have the high fatigue resistance against light irradiation. We believe that PABI derivatives become a widely applicable photoswitching system in the field of fundamental research and practical applications.

This work was supported partly by the Core Research for Evolutional Science and Technology (CREST) program of the Japan Science and Technology Agency (JST) and a Grant-in-Aid for Scientific Research (A) (22245025) from Ministry of Education, Culture, Sports, Science and Technology (MEXT), Japan.

Notes and references

^a Department of Chemistry, School of Science and Engineering, Aoyama Gakuin University, 5-10-1 Fuchinobe, Chuo-ku, Sagami-hara, Kanagawa 252-5258, Japan.

E-mail: jjiro_abe@chem.aoyama.ac.jp; Fax: +81-42-759-6225;

Tel: +81-42-759-6225

^b CREST, Japan Science and Technology Agency, K's Gobancho, 7 Gobancho, Chiyoda-ku, Tokyo 102-0076, Japan.

† Electronic Supplementary Information (ESI) available: Experimental details and characterization data. See DOI: 10.1039/c000000x/

1. T. Hayashi and K. Maeda, *Bull. Chem. Soc. Jpn.* 1960, **33**, 565–566.
2. D. M. White and J. Sonnenberg, *J. Am. Chem. Soc.* 1966, **88**, 3825–3829.
3. R. Cohen, *J. Org. Chem.* 1971, **36**, 2280–2284.
4. J. Abe, T. Sano, M. Kawano, Y. Ohashi, M. M. Matsushita, and T. Iyoda, *Angew. Chem. Int. Ed.* 2001, **40**, 580–582.

5. M. Kawano, T. Sano, J. Abe, and Y. Ohashi, *J. Am. Chem. Soc.* 1999, **121**, 8106–8107.
6. K. Shima, K. Mutoh, Y. Kobayashi, and J. Abe, *J. Am. Chem. Soc.* 2014, **136**, 3796–3799.
7. T. Yamaguchi, S. Hatano, and J. Abe, *J. Phys. Chem. A* 2014, **118**, 134–143.
8. K. Mutoh, K. Shima, T. Yamaguchi, M. Kobayashi, and J. Abe, *Org. Lett.* 2013, **15**, 2938–2941.
9. S. Hatano, T. Horino, A. Tokita, T. Oshima, and J. Abe, *J. Am. Chem. Soc.* 2013, **135**, 3164–3172.
10. H. Yamashita and J. Abe, *J. Phys. Chem. A* 2011, **115**, 13332–13337.
11. K. Mutoh and J. Abe, *Chem. Commun.* 2011, **47**, 8868–8870.
12. K. Mutoh and J. Abe, *J. Phys. Chem. A* 2011, **115**, 4650–4656.
13. S. Hatano, K. Fujita, N. Tamaoki, T. Kaneko, T. Nakashima, M. Naito, T. Kawai, and J. Abe, *J. Phys. Chem. Lett.* 2011, **2**, 2680–2682.
14. A. Kimoto, A. Tokita, T. Horino, T. Oshima, and J. Abe, *Macromolecules* 2010, **43**, 3764–3769.
15. Y. Harada, S. Hatano, A. Kimoto, and J. Abe, *J. Phys. Chem. Lett.* 2010, **1**, 1112–1115.
16. Y. Kishimoto, and J. Abe, *J. Am. Chem. Soc.* 2009, **131**, 4227–4229.
17. K. Fujita, S. Hatano, D. Kato, and J. Abe, *Org. Lett.* 2008, **10**, 3105–3108.
18. N. Ishii, T. Kato, and J. Abe, *Sci. Rep.* 2012, **2**, 819.
19. N. Ishii and J. Abe, *J. Appl. Phys.* 2013, **102**, 163301.
20. K. Mutoh, M. Sliwa, and J. Abe, *J. Phys. Chem. C* 2013, **117**, 4808–4814.
21. K. Okada, K. Imamura, M. Oda, M. Kozaki, Y. Morimoto, K. Ishino, and K. Tashiro, *Chem. Lett.* 1998, 891–892.
22. K. Okada, K. Imamura, M. Oda, A. Kajiwara, M. Kamachi, K. Ishino, K. Tashiro, M. Kozaki, K. Sato, and T. Takui, *Synth. Met.* 1999, **103**, 2308–2309.
23. U. Mayer, H. Baumgärtel, and H. Zimmermann, *Angew. Chem.* 1966, **78**, 303–303.
24. A. Kikuchi, F. Iwahori, and J. Abe, *J. Phys. Chem. B* 2005, **109**, 19448–19453.
25. A. Kikuchi and J. Abe, *Chem. Lett.* 2005, 1552–1553.
26. D. Döhnert and J. Koutecky, *J. Am. Chem. Soc.* 1980, **102**, 1789–1796.
27. C. R. Flynn and J. Michl, *J. Am. Chem. Soc.* 1974, **96**, 3280–3288.
28. A. A. Ovchinnikov, *Theor. Chim. Acta* 1978, **47**, 297–304.
29. J. L. Segura and N. Martín, *Chem. Rev.* 1999, **99**, 3199–3246.
30. N. Martin, C. Seoane, and M. Hanack, *Org. Prep. Proced. Int.* 1991, **23**, 237–272.
31. J. L. Charlton and M. M. Alauddin, *Tetrahedron* 1987, **43**, 2873–2889.
32. M. Szwarc, *Nature* 1947, **160**, 403.
33. A. K. Sadana, R. K. Saini, and W. E. Billups, *Chem. Rev.* 2003, **103**, 1539–1602.
34. A. Kikuchi, F. Iwahori, and J. Abe, *J. Am. Chem. Soc.* 2004, **126**, 6526–6527.
35. C. Che, S. Li, Z. Yu, F. Li, S. Xin, L. Zhou, S. Lin, and Z. Yang, *ACS Comb. Sci.* 2013, **15**, 202–207.
36. Crystallographic data for (a) **1aL**: $\text{C}_{36}\text{H}_{26}\text{N}_4$, $M_r=514.61$; triclinic; space group $P\bar{1}$; $a=9.0514(11)$, $b=12.8065(11)$, $c=12.8890(15)$ Å; $\alpha=98.181(1)^\circ$, $\beta=107.151(1)^\circ$, $\gamma=103.624(1)^\circ$; $V=1350.9(3)$ Å³; $\rho_{\text{calcd}}=1.260$ g cm⁻³; $Z=2$; $R_1=0.0459$ [$I > 2.0\sigma(I)$], $wR_2=0.0660$ (all

data), GOF=1.322 (data/restrain/params=5844/0/370). CCDC 999576 contains the supplementary crystallographic data for this paper.; (b) **1a**: C₃₆H₂₄N₄, M_r=512.59; orthorhombic; space group *Pna*2₁; *a*=15.8279(16), *b*=13.8209(7), *c*=14.2201(7) Å; $\alpha=90$, $\beta=90$, $\gamma=90^\circ$; *V*=2693.1(5) Å³; $\rho_{\text{calcd}}=1.264$ g cm⁻³; *Z*=4; *R*₁=0.0396 [*I* > 2.0σ(*I*)], *wR*₂=0.0890 (all data), GOF=1.034 (data/restrain/params=4290/1/362). CCDC 999577 contains the supplementary crystallographic data for this paper. These data can be obtained free of charge from The Cambridge Crystallographic Data Center via www.ccdc.cam.ac.uk/data_request/cif.

37. H. E. Simmons and T. Fukunaga, *J. Am. Chem. Soc.* 1967, **89**, 5208–5215.
38. R. Hoffmann, A. Imamura, and G. D. Zeiss, *J. Am. Chem. Soc.* 1967, **89**, 5215–5220.